We are IntechOpen, the world's leading publisher of Open Access books Built by scientists, for scientists

4,800
Open access books available

122,000
International authors and editors

135M
Downloads

Our authors are among the

154
Countries delivered to

TOP 1%
most cited scientists

12.2%
Contributors from top 500 universities

WEB OF SCIENCE™

Selection of our books indexed in the Book Citation Index in Web of Science™ Core Collection (BKCI)

Interested in publishing with us?
Contact book.department@intechopen.com

Numbers displayed above are based on latest data collected.
For more information visit www.intechopen.com

1

Atmospheric Low Frequency Variability: The Examples of the North Atlantic and the Indian Monsoon

Abdel Hannachi[1], Tim Woollings[2] and Andy Turner[3]
[1]*Department of Meteorology, Stockholm University, Sweden*
[2]*Department of Meteorology, University of Reading*
[3]*NCAS-Climate, Walker Institute for Climate System Research, Department of Meteorology, University of Reading*
[1]*Sweden*
[2,3]*UK*

1. Introduction

Great efforts, sometimes taking the form of a race, are exerted by climate scientists to provide medium and long-term future climate predictions on large and regional, or even local scales. This exercise has proved to be a really challenging one. There is a wide variety of climate characteristics between different regions on the globe. For example, tropical and subtropical regions tend to be more influenced by what happens in the equatorial Indian and Pacific oceans such as the El Nino Southern Oscillation (ENSO). Midlatitude regions, on the other hand, are more affected by the north-south migration of the polar front or synonymously the midlatitude jet stream. It is important to notice that even within the midlatitude band climate variation differs from region to region. For example, climate variability over the North Atlantic European region is different from that of the Pacific North America (PNA) region and is particularly more difficult to predict.

The jet stream is a belt of strong westerly wind that goes around the globe in the subtropics (subtropical jet) or the midlatiudes (eddy-driven jet). The subtropical jet results from the westerly acceleration of poleward moving air associated with the upper branch of the Hadley cell. The midlatitude jet stream, on the other hand, results from the momentum and heat forcing by midlatitude eddies, i.e. weather systems. Weather and climate variations in the extratropics are associated to a large extent with meridional shifts of the midlatitude westerly jet stream. For instance, major extratropical teleconnections, including the North Atlantic Oscillation (Fig. 1) and the PNA pattern, describe changes in the jet stream (Wittman et al. 2005; Monahan and Fyfe 2006). Over the North Atlantic region, the North Atlantic Oscillation (NAO) is the dominant large scale mode of variability with its north-south dipole anomaly centres (Hurrell et al. 2002). It is a seesaw in atmospheric mass between the subtropical high and and the polar low and affects much of the weather and climate in the North Atlantic, east of North America, Europe and parts of Russia. The positive phase of the NAO (Fig. 1b) is generally associated with a stronger subtropical high pressure and a deeper than normal

Icelandic low yielding warmer and wetter, than normal, conditions over Europe associated with colder and drier, than normal, conditions in northern Canada and Greenland. The negative phase (Fig. 1a) is the opposite of the positive phase and yields moist air into the Mediterranean and cold air in northern Europe.

The second prominent mode of variability over the North Atlantic-European region is the East Atlantic (EA) pattern. The EA pattern also has a north-south dipole of anomaly centres that are displaced southward with respect to those of the NAO so that both patterns are in quadrature and the northern centre, centered around 45^{o}N, is stronger than the lower latitude centre, which is more linked to the subtropics and modulated by the subtropical ridge. The positive phase of the EA is associated with above- and below-average surface temperature over Europe and eastern North America respectively. The variability of these modes is usually described by patterns in pressure or geopotential height fields, or wind fields as in Athanasiadis et al. (2009). Jet stream shifts are associated with a positive feedback between the mean flow and the transient eddies (eg, Lorenz and Hartmann 2003).

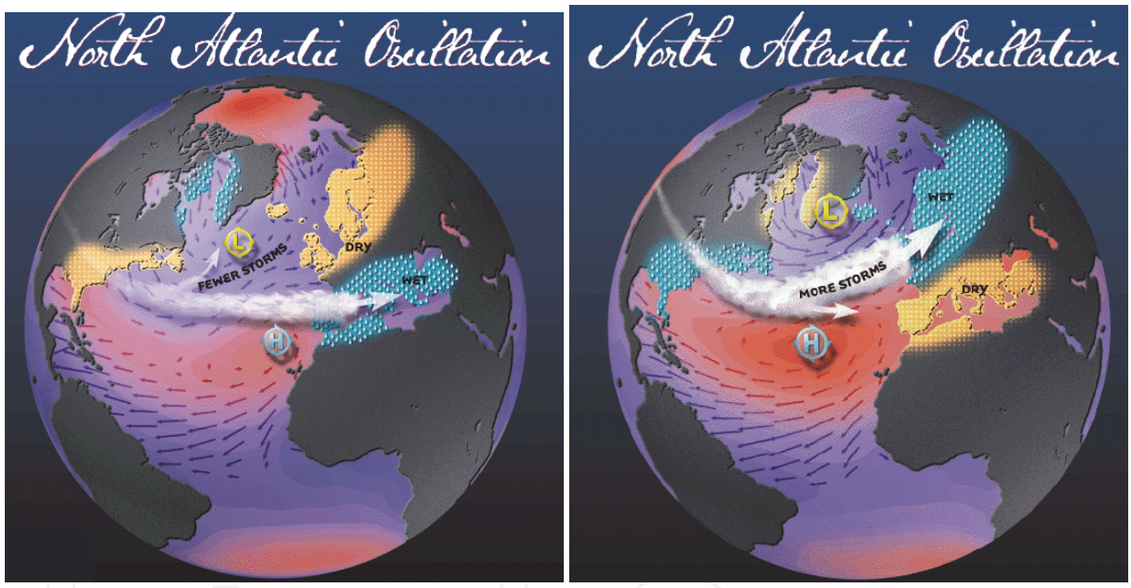

(a) Negative NAO (b) Positive NAO

Fig. 1. Illustration of the negative (a) and positive (b) phases of the NAO pattern in terms of winds, moisture and surface temperature. Source: http://www.ldeo.columbia.edu/res/pi/NAO/.

Woollings et al. (2010a, WO10a hereafter) analysed the variability of the leading mode of the 500-hPa geopotential height (Z500) derived from the 44 winters (December-February, DJF) 1957/58-2000/01 of the 40-year European Centre for Medium-Range Weather Forecasts (ECMWF) Re-Analysis (ERA-40) (Uppala et al. 2005). They suggested that the NAO can be interpreted in terms of a transition between two states; a high-latitude (Greenland) blocking and a no blocking flow. The complex behaviour of the jet stream variability means that it requires at least two spatial patterns to describe its dominant variations (Fyfe and Lorenz 2005; Monahan an Fyfe 2006), and for the North Atlantic these are the NAO and the EA

patterns (Woollings et al. 2010b). Woollings et al. (2010b, WO10b hereafter) considered the winter (DJF) ERA-40 low-level (925-700 hPa) wind to analyse the latitude and speed of the eddy-driven jet stream. Their analysis suggests, as it is also described below, that there are three preferred latitudinal positions of the North Atlantic jet stream, and this is in very good agreement with similar flow structures obtained from a Gaussin mixture model applied to the two-dimensional (NAO,EA) state space. Two of the jet positions are found to be associated with the two states identified in WO10a, and which reflect the NAO variability.

Climate is by definition a high dimensional and complex system involving highly nonlinear interacting processes. Nonlinearity means, in particular, that changes in climate due to changes in external forcing, such as greenhouse gases, do not scale linearly with the latter and surprises are expected to occur. Weather and climate variability is not pure randomness but embeds some sort of dynamical structure. In synoptic meteorology, for example, it has been the practice to regard weather and climate variability as consisting of a small number of large scale weather patterns, also known as weather regimes, that reccur intermittently hence affecting regional climate through their persistence and integrating effect. Persistence and meridional shifts of the jet stream could therefore hold the key to any regime-like behaviour. Under climate warming these regimes are expected to change by changing their structure and/or their frequency of occurrence (Palmer Palmer 1999; Branstator and Selten 2009). These changes can have serious impacts on the economy and society. For example, under global warming it is projected that deserts and areas susceptible to drought will increase. In the meantime extreme precipitation events, which often damage crops, and (summer) heat waves, which cause health problems, will become more frequent.

In the tropics different processes are involved. For the monsoons, for example, the fundamental driving mechanisms are differential heating between sea and land masses and moisture transport. One of the main regions of monsoon activity on Earth is the Asian monsoon region. The Asian summer monsoon is very important not least for affecting the lives of more than the third of the world's population. While seasonal mean Asian monsoon is reasonably well understood through lower-boundary forcings (Charney and Shukla 1981), subseasonal (30-60 day timescale) variations of monsoon or monsoon intraseasonal variability (MISV), generally linked to what is commonly known as active and break monsoon phases, is less so. Although MISV tends to be more chaotic there is evidence suggesting increased frequency of active (break) conditions during strong monsoon (drought) years.

This chapter reviews and discusses the state-of-the-art of climate variability and nonlinearity in the midlatitude and the tropical regions based on the works of Woollings et al. (2010b) and Turner and Hannachi (2010, TH10). We show, in particular, the similarirty between the two regions in terms of nonlinearity and the possible effect of global warming using ERA-40 reanalyses. The first region is the winter North Atlantic European sector characterised by its midlatitude climate (WO10b). The second one is the summer monsoon region around India and South East Asia (TH10). Both regions are found to be characterised by nonlinear regime behaviour. The study applies mixture model techniques (Hannachi and Turner 2008; TH10; WO10b) to the jet latitude index and the NAO/EA teleconnection patterns in one case and to a simple index of the Asian summer monsoon convection derived from the ERA-40 reanalysis in the other. Section 2 describes the data and methodology. Section 3 discusses the case of the North Atlantic/European region and section 4 discusses the Asian summer monsoon case. A summary and a discussion are presented in the last section.

2. Data and methodology

2.1 Data

We have used the 500-hPa geopotential height (Z500) data from the ERA-40 reanalysis project (Uppala et al. 2005). The gridded data are defined on a regular $2.25^o \times 2.25^o$ grid north of 20^oN and span the period December−February (DJF) 1957/58−2000/01 yielding 44 complete winter (DJF) seasons. Daily and monthly data are used. A smooth seasonal cycle is obtained by averaging daily data over all the years then smoothing with a discrete cosine transform retaining only the mean and the lowest two Fourier frequencies. Daily anomalies are obtained by subtracting the smooth seasonal cycle from the original daily data.

For the Asian monsoon, we have used the outgoing long-wave radiation (OLR) and 850-mb wind fields from ERA-40 (Uppala et al. 2005) over the Asian summer monsoon region $(50 - 145E, 20S - 35N)$ for the period 1958-2001. Daily detrended anomalies are obtained by removing the seasonally-varying mean field based on monthly averages. The monsoon season is defined by the months June-September (JJAS). In addition, to characterise the large scale seasonal mean influence on monsoon convection we have used the dynamical monsoon index (WY) proposed by Webster and Yang (1992). The WY index is a proxy for the (adiabatic) heating of the atmospheric column and is defined as the JJAS average of anomalous zonal wind shear between the lower (850-hPa) and upper (200 hPa) tropospheric levels averaged over the band $(40 - 110E, 5 - 20N)$. We also used the daily India Meteorological Department rainfall gridded data (Rajeevan et al. 2006) as an independent measure of monsoon rainfall (see TH10 for more details).

2.2 Methodology

The jet-latitude index (WO10b) is computed for the period 1 December 1957 − 28 February 2002 by averaging daily mean zonal winds over the levels 925, 850, 775 and 700 hPa and the longitudes $0 - 60^o$W. A 10-day low-pass Lanczos filter is then applied to the data and the maximum wind speed value is used to define the jet latitude and speed. A smooth seasonal cycle is then removed from these to give anomaly values (see WO10b for more details). The NAO and EA patterns and associated indices are obtained as the leading empirical orthogonal functions (Hannachi et al. 2007) of Z500 anomalies over the Atlantic sector $(20^o - 90^o N, 90^o W - 90^o E)$, see WO10a and WO10b for details.

To estimate the probability density function (PDF) function we used the unidimensional kernel density estimation method (Silverman 1981). In addition we have also used the univariate and multivariate mixture model approach (Hannachi 2007; WO10b; TH10). In this model, the PDF is decomposed as a weighted sum of Gaussian (univariate and multivariate) normal PDFs. The centre and the covariance structure of each Gaussian component from the mixture is then analysed separately.

3. North Atlantic jet and atmospheric circulation

As we have mentioned in the introduction, the NAO is the dominant mode of weather and climate variability over the North Atlantic sector. WO10a showed that the NAO can be explained as a transition between two flow states (Fig. 2); a Greenland blocking (GB), associated with a negative NAO phase, and a no-blocking flow, looking like a split jet and is associated with a positive phase of the NAO. Croci-Maspoli (2007) showed, in fact, that when all blocking events were removed from the ERA40 the NAO is no longer the leading empirical

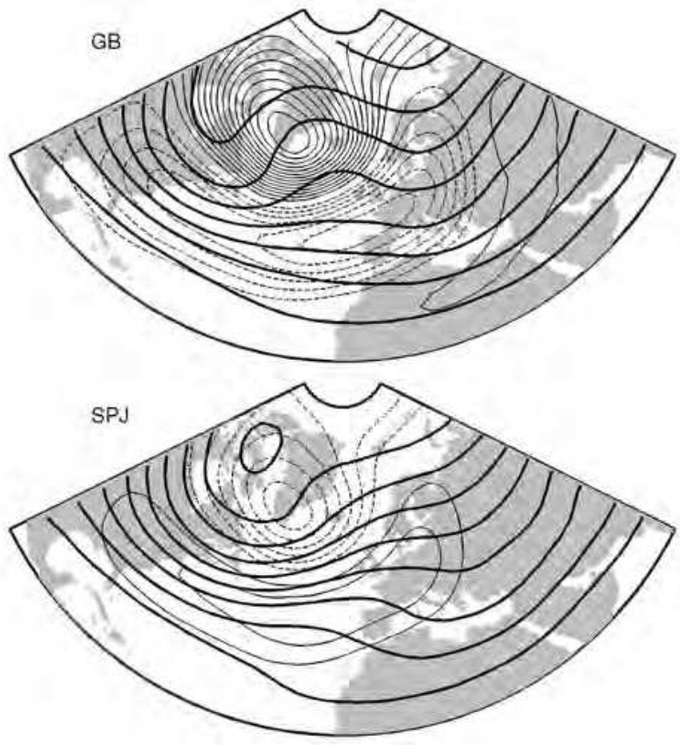

Fig. 2. Flow regimes of the full (thick contours) and anomaly (thin contours) of the winter (DJF) ERA-40 Z500 field obtained from the mixture model applied to the NAO time series. Contour intervals: 100 m (full field) and 10 m (anomalies). Negative contour dashed (reproduced from WO10a)

orthogonal function or EOF (Hannachi et al. 2007). Since much of the weather and climate variability of the extratropics is associated with the jet stream variability it is expected that the flow states or regimes must be associated somehow with particular structures of the jet. WO10b identified the eddy-driven jet stream by computing the jet latitude and the associated maximum wind.

Figure 3 shows an example of the time evolution of the jet latitude for the four winters (DJF) 1957/1958 to 1960/1961 of the zonal wind computed over the North Atlantic region. The jet latitude is characterised by periods of persistence at specific latitudes[1] and periods of transitions between these latitudes. This indicates that the jet stream is characterised by persistence in addition to north-south migration. An extended period of the jet evolution over 8 winters Dec 1958 - Feb 1967 is shown in Fig. 4a as a time series. To identify the persistence locations of the eddy-driven jet stream Fig. 4b shows the kernel PDF of the jet latitude along with the same PDF estimated using the mixture model. The jet latitude PDF clearly has a trimodal structure reflecting three preferred locations for the North Atlantic eddy-driven jet stream shown by the dotted lines in Fig. 3.

The Z500 anomaly flow patterns associated with the peaks of the jet latitude PDF are shown in Fig. 5 based on compositing over the closest 300 days to these peaks. The left hand side peak corresponds to the southern jet regime characterised by its high pressure or blocking over

[1] shown by the dotted lines in Fig. 3 and are discussed later

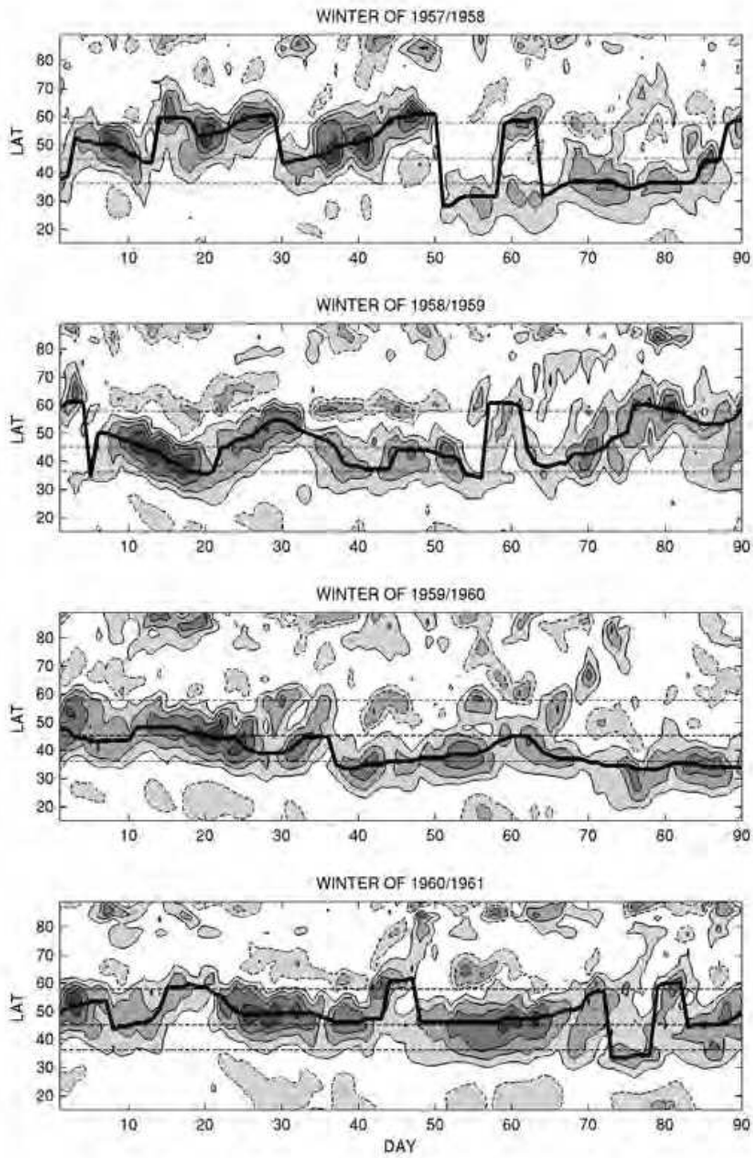

Fig. 3. Daily zonal-mean zonal-wind averaged over longitudes $0 - 60^{o}$W and pressure levels 925-700 hPa versus time for the first four years of ERA-40 winters (DJF 1957/1961). The jet latitude is shown by the thick line and the preferred jet latitudes are shown by dashed horizontal lines. Contour interval 5 m/s, and negative contours dashed.

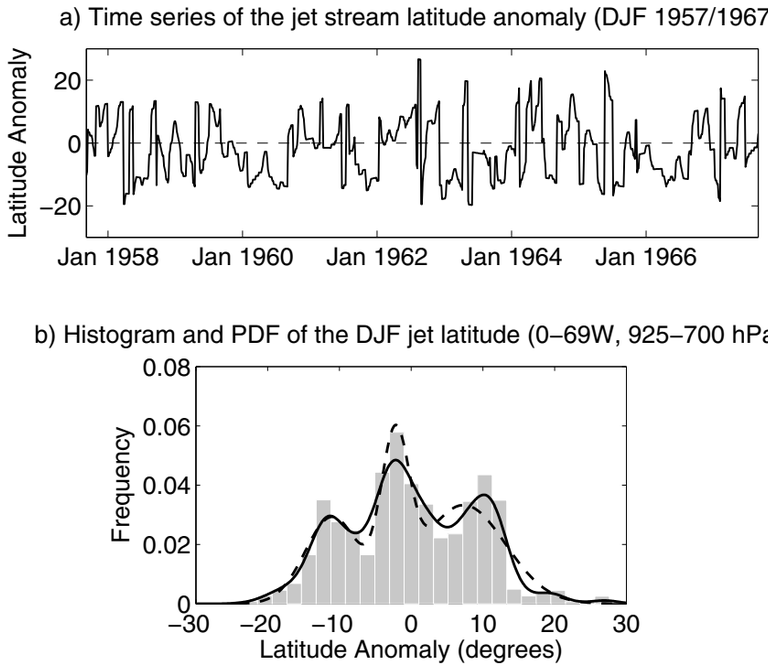

Fig. 4. A segment of the jet latitude time series for the first 10 winters (DJF 1957/1967) of ERA-40 (a), and the histogram along with the kernel (continuous) and mixture model (dashed) PDF estimate (b). Reproduced from Hannachi et al. (2012).

Greenland. The middle peak is associated with a low pressure centre over the midlatitude North Atlantic whereas the right hand side peak corresponds to a high pressure over the midlatitude North Atlantic. The southern jet position is similar to the negative NAO phase whereas the middle and north jet regimes look more like the opposite phases of the EA pattern. A similar composite applied to the zonal wind (not shown) indicates that only for the central and north jet composites is the eddy-driven jet stream separated from the subtropical jet (WO10b).

To link the jet variation to the low frequency variability in the North Atlantic/European sector we consider next the state space of the winter (DJF) daily Z500 anomalies, and we follow WO10b by using the leading two modes of variability, i.e. the NAO and the EA patterns. Fig. 6 shows a scatter plot of the data color-coded to show the latitude (anomaly) of each day. The mixture model is applied as in WO10b to this scatter plot using three bivariate Gaussian components each characterised by its centre (or mean) and its covariance matrix.

The ellipses in Fig. 6 reflect the covariance structure of the different bivariate components and the small filled circles represent their centres. The projection onto the NAO-EA plane of the patterns shown in Fig. 5 are indicated by crosses and they are quite close to the centres of the mixture components. In addition the ellipses are also in very good agreement with the colors of the data points (Fig. 6). The Z500 anomaly maps of the centres of the mixture model are shown in Fig. 7. These regimes are very similar to the composites of the jet regimes shown in Fig. 5.

It is clear that the low-frequency flow regimes over the North Atlantic sector are associated to the persistent states of the eddy-driven jet stream. The southern jet position is explained by the persistent GB blocking. The central position seems to be related to the undisturbed state

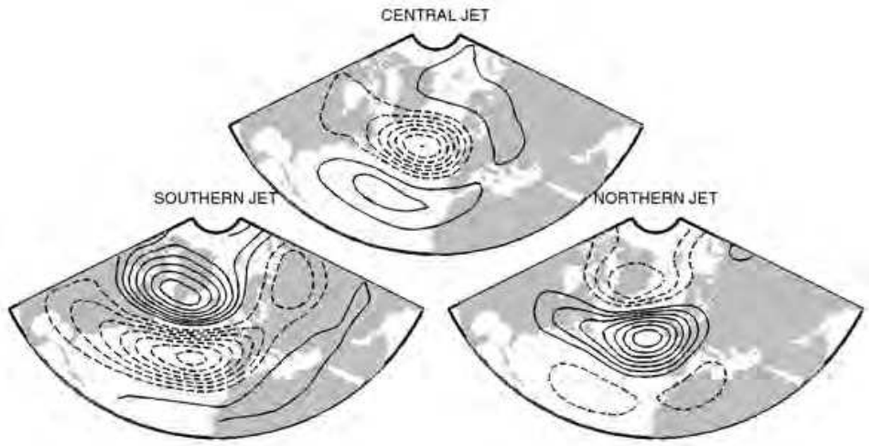

Fig. 5. 500mb geopotential height maps corresponding to the three PDF peaks of the jet latitude. Contour interval 20 m, negative contours dahed and zero contour omitted. Reproduced from WO10b.

of the jet given its proximity to the mode (or peak) of the two dimensional Gaussian mixture distribution (not shown). As for the northern jet position, it only partly reflects the occurrence of blocking in the southwest of Europe, which could divert the jet northward (Woollings et al. 2011).

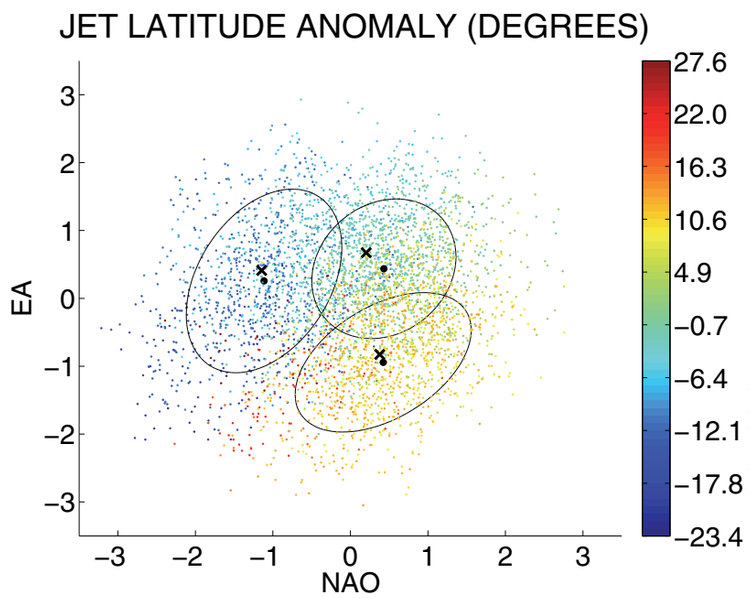

Fig. 6. Scatter plot of the daily winter (DJF) Z500 anomalies, projected onto the NAO/EA plane and color-coded to show the jet latitude. The ellipses and their associated centres correspond respectively to the covariances and the means of the Gaussian component mixture model. The crosses represent the regimes obtained from the jet latitude PDF projected onto the same plane (reproduced from WO10b).

An important issue arises in climate variability in relation to global warming, and that is the following. How will weather and climate variability look like in a warmer future? This

is an important question for strategic planning. The available reanalyses data are generally limited to less than 100 years, including the ERA-40, which is only about 50 years long, and therefore cannot be used to give a definite answer to the above question. We have, never the less, attempted to look at this question by splitting the jet latitude time series into pre- and post-1978 subsamples and looked at the respective PDFs. The result (not shown) indicates that the trimodal structure is conserved between the two periods. There is, however, a significant decrease of the southern jet regime frequency in the last half of the record compared to the first half. This is concomitant with a decrease of Greenland blocking frequency. We reiterate again that, given the length of the data, this could simply reflect the natural variability rather than an anthropogenic trend.

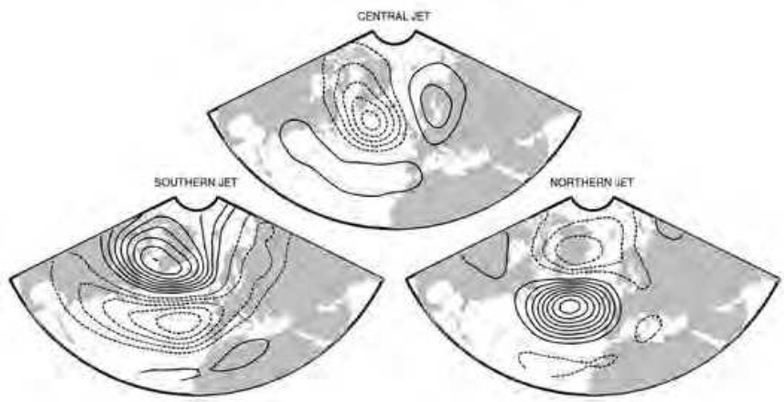

Fig. 7. As in Fig. 5 but for the centres of the Gaussian components of the mixture model. Reproduced from WO10b.

There is also a slight increase of frequency of the central and northern jet frequency. As for the latitudinal shift there is a slight hint of a northward shift of the jet latitude PDF peaks although it is not significant. Climate change studies based on the climate model intercomparison project (CMIP3) models (Barnes and Hartmann 2010) do indicate indeed a northward shift of the jet stream in warmer climate. Despite the rather large differences between the climate models of the CMIP experiment the northward shift of the jet stream seems to be a robust feature.

4. Asian monsoon variability

The OLR is a proxy for convection and we use it here to discuss the MISV over the Asian summer monsoon region. The leading EOF of the OLR anomalies explain about 24% of the total variance and is well separated from the variances of the rest of the modes of variability and we discuss the MISV based on this mode of variability following TH10. Figure 8a shows the OLR EOF1 with its dipolar structure showing opposite variability between the maritime continent and parts of India and south China. The first principal component (PC1) associated with EOF1 (Fig. 8a) is used to analyse MISV. Fig. 8b shows the PDF of the index along with the two Gaussian components used in the two-component mixture model.

The left hand side regime R1 (Fig. 8b) is clearly associated with the opposite phase of the EOF1 pattern (Fig. 8a), i.e. a negative phase of OLR over southern India associated with a positive phase over the maritime continent. The composites of daily 850-mb wind and OLR

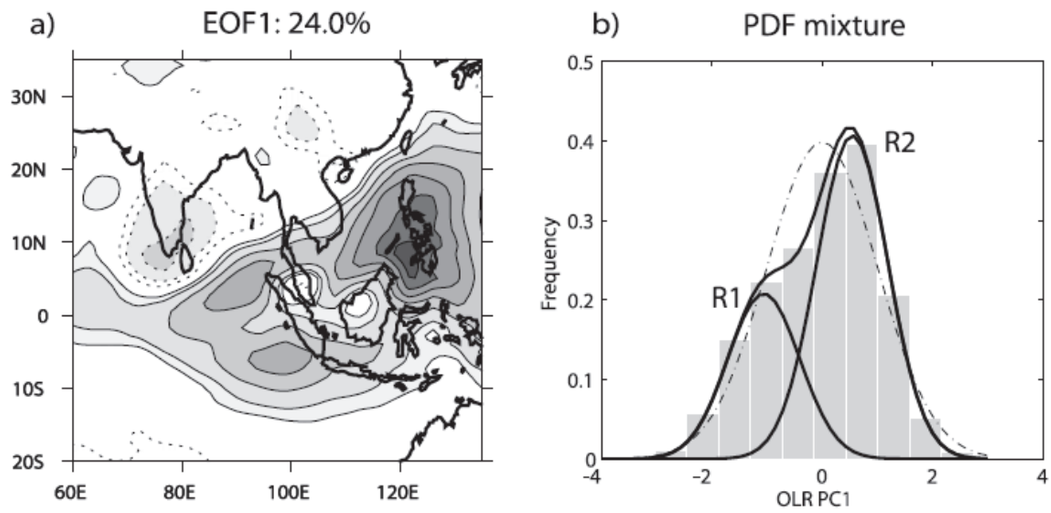

Fig. 8. (a) Leading empirical orthogonal function of JJAS ERA-40 OLR anomalies for the period 1958-2001. (b) Probability density function (upper solid curve) of the OLR index and the associated two Gaussian components of the mixture model (lower solid curves, indicated by R1 and R2). The dashed-dotted curve represents the Gaussian PDF fitted to the index. In (a) the contour interval is arbitrary and positive (negative) contours are dotted (continuous) (reproduced from TH10).

anomaly fields based on days close to the PDF mode corresponding to the left regime R1 (Fig. 8b) are shown in Fig. 9a. A similar composite of rainfall for the same regime R1 is shown in Fig. 9b. The regime flow R1 is consistent with an anticyclonic circulation over the maritime continent and south China sea with a reversal of the Somali jet and a diversion northward with convergence over most of the southern part of India. The composite map of rainfall (Fig. 9b) clearly shows a positive precipitation anomaly consistent with the monsoon active phase. The second regime R2 (Fig. 8b) has an opposite OLR phase to that of R1 with a positive OLR phase over southern India and a negative phase over the maritime continent. The wind field composite (Fig. 9c) shows a divergent flow over india and eastern Bay of Bengal and a cyclonic circulation over the Philippines and South China sea. The OLR amplitudes (Fig. 9c) are smaller than those of R1, with about 5 w/m^2 vs 15 w/m^2 over southern India and the Philippines respectively. The wind field is also weaker with a southward shift of the Somali jet. The map of rainfall composites (Fig. 9d) shows dry conditions over India consistent with a break phase of the Summer Asian monsoon. The robustness of the active and break phases has been tested in TH10, to which the reader is referred for more details.

The trend analysis of MISV was investigated by comparing monsoon activity between the first and second halves of ERA-40 data (TH10). The results indicate that the active monsoon has been reduced whereas the break phase has become more frequent in the second half (Fig. 10a). The relationship between the intraseasonal monsoon and the large-scale seasonal mean monsoon was also addressed by TH10 using the Webster-Yang (WY) index. We found that MISV is closely related to the large-scale monsoon variability (Fig. 10b). Precisely, seasons with above-normal monsoon heating the break and active phases have equal likelihood. On the other hand, seasons with below-normal large-scale monsoon heating the break phase becomes more likely.

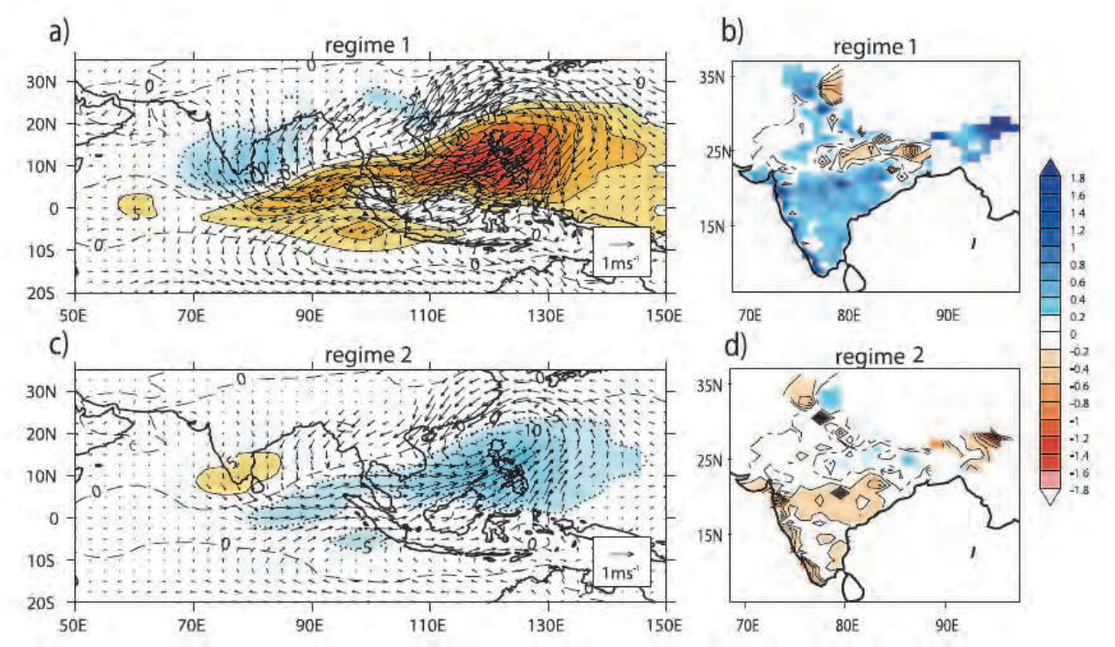

Fig. 9. Composite anomalies of OLR and wind field and rainfall over India for the first (a,b) and second (c,d) monsoon regimes over the 1958-2001 period. Contour interval for OLR composites is 5 wm^{-2}, red solid (blue dotted) is positive (negative). Rainfall contours are 0.2 mm/day, and negative contour lines only are shown (reproduced from TH10).

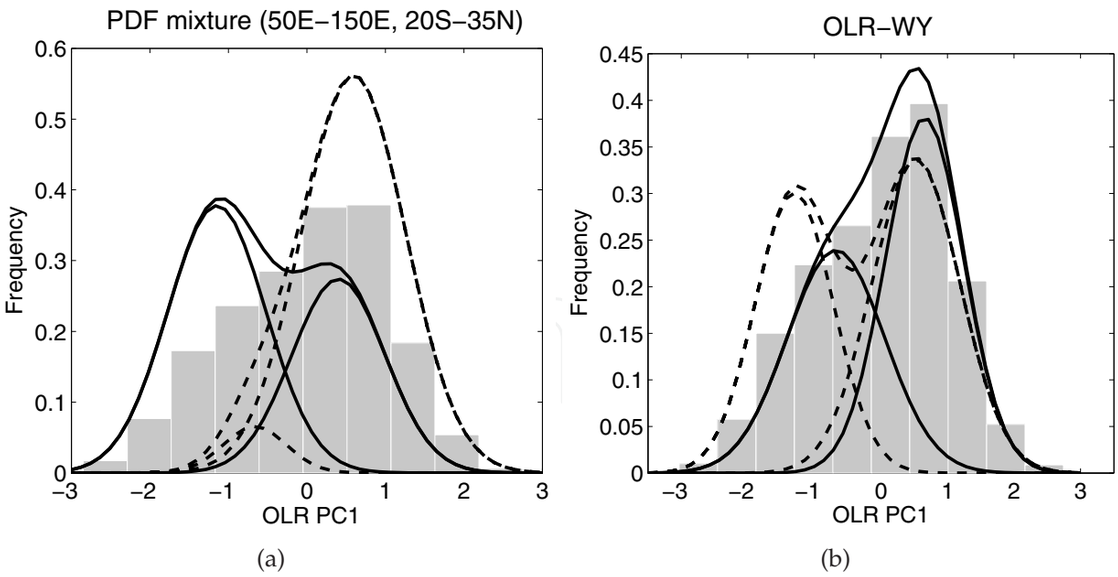

(a) (b)

Fig. 10. (a) PDFs of the daily OLR time series in the early (solid) and late (dahsed) part of the record. Upper (lower) curves represent total (mixture components) probability distributions. The left (right) component of the mixture represents regime R1 (R2). (b) Perturbations to the whole period mixture when the OLR index is stratified by JJAS-average dynamical monsoon, or Webster-Yang, index: WY^{+} (dashed) and WY^{-} (solid). Reproduced from TH10.

5. Summary and conclusion

We have reviewed in this chapter some specific characteristics relating to the nature of the large scale and low-frequency atmospheric variability. The discussion focussed essentially on the nonlinear nature governing this variability. Two important regions are discussed in this chapter, one in the midlatitudes and the other in the tropics. The first region is the North Atlantic/European sector and the discussion follows Woollings et al. (2010b). The second region is the summer monsoon Asia, and the discussion follows Turner and Hannachi (2010). The data used come from the ECMWF and consist of the ERA-40 winter (DJF) geopotential height, zonal wind from the lower troposphere, over the North Atlantic sector as well as the 850 mb horizontal wind and sea level pressure over the Asian summer (JJAS) monsoon region. In the extratropics well-documented prominent modes of variability are known to control the climate variability. The North Atlantic Oscillation, a north-south seeesaw in the atmospheric mass, and also the East Atlantic pattern constitute major contributors to weather and climate variation in the North Atlantic/European region. For the NAO pattern, for example, various mechanisms have been proposed to explain its existence. WO10a, for example, suggested that the NAO is the consequence of regime transitions between the two flow patterns; a Greenland blocking and a no-blocking flow. Weather and climate variability in the extratropics can be explained by variation, such as meriodinal shift, of the midlatitude westerly jet stream. It is therefore natural to seek an explanation of the low-frequency and large-scale flow patterns in the North Atlantic sector based on the midlatitude or eddy-driven jet stream variability.

A jet latitude index was compued by WO10b, based on the maximum of the zonal mean zonal wind averaged over the North Atlantic sector and the four lowest pressure levels of ERA-40. The PDF of the jet latitude was then computed and revealed a trimodal structure. The modes represent three latitudinal positions of the eddy-driven jet stream. The first one represents the southern jet position, situated around latitude 36^oN, and is associated with the Greenland blocking. The next one represents the middle jet position around 45^oN, and the last one represents the jet when it is at its northern most latitude, around 57^oN.

These jet locations have been linked to the weather and climate variability over the sector. Using the reduced state space spanned by the two leading modes of variability, the NAO and EA patterns, of the 500-mb geopotential height, the mixture model yields three regimes very similar to those associated with the peaks of the jet latitude PDF. A simple analysis based on comparing the jet latitude time series between the two halves of the ERA-40 record reveals a significant reduction of the frequency of the southern jet regime as we go from the first to the second half of the data record. In addition, there is a northward shift, albeit small, of the jet stream location.

The same analysis, based on the mixture model, was also applied to the time series of the first OLR EOF over the Asian monsoon region. Two phases of the intraseasonal monsoon variability were identified, which are consistent with the break and active monsoon phases over India. The seasonal mean condition is then found to affect the likelihood of these regimes providing evidence that large scale forcing can lend some predictability to monsoon weather patterns during the season. For example, seasons with above-normal monsoon heating can yield equal likelihood for both intraseasonal monsoon phases. The trend analysis of intraseasonal monsoon activity also reveals an increase of the break phase at the expense of the active phase. A more detailed analysis of these issues is, however, beyond the scope of this chapter and is left for future research.

6. Acknowledgements

We thank ECMWF for providing the ERA-40 reanalysis data.

7. References

Athanasiadis, P. J.; Wallace, J. M., & J. J. Wettstein, J. J. (2009). Patterns of jet stream wintertime variability and their relationship to the storm tracks. *Journal of the Atmospheric Sciences*, Vol., 67, 1361–1381.

Barnes, E. A. & Hartmann, D. L. (2010). Influence of eddy-driven jet latitude on North Atlantic jet persistence and blocking frequency in CMIP3 integrations. *Geophysical Research Letters*, Vol., 37, doi:10.1029/2010GL045700.

Branstator, G. & Selten, F. (2009). "Modes of Variability" and Climate Change. *Journal of Climate*, Vol., 22, 2639–2658.

Charney, J. G. & Shukla, J. (1981). Predictability of monsoons, in Sir Lighthill, J.; & Pearce, R. P. (ed.), *Monsoon Dynamics*, Cambridge University Press, pp. 99–109.

Croci-Maspoli, M.; Schwierz, C. & Davies, H. C. (2007). Atmospheric blocking: Space-time links to the NAO and PNA. *Climate Dynamics*, Vol, 29, 713–725.

Fyfe, J. C. & Lorenz, D. J. (2006). Characterizing midlatitude jet variability: lessons from a simple GCM. *Journal of Climate*, Vol, 18, 3400–3404.

Hannachi, A.; Jolliffe, I. T. & Stephenson, D. B. (2007). Empirical orthogonal functions and related techniques in atmospheric science: A review. *International Journal of Climatology*, Vol, 27, 1119–1152.

Hannachi, A. (2007). Tropospheric planetary wave dynamics and mixture modeling: Two preferred regimes and a regime shift. *Journal of the Atmospheric Sciences*, Vol, 64, 3521–3541.

Hannachi, A. & Turner, A. G. (2008). Preferred structures in large scale circulation and the effect of doubling greenhouse gas concentration in HadCM3. *Quarterly Journal of the Royal Meteorological Society*, Vol, 134, 469–480.

Hannachi, A.; Woollings, T. & Fraedrich, K. (2012). The North Atlantic jet stream: A look at preferred positions, paths and transitions. *Quarterly Journal of the Royal Meteorological Society*, in press.

Hurrell, J. W.; Kushnir, Y.; Ottersen, G. & Visbeck, M. (2002). An overview of the North Atlantic Oscillation. In *The North Atlantic Oscillation−Climate Significance and Environmental Impact*, Geophysical Monograph, Vol, 134, American Geophysical Union, 1–35.

Lorenz, D. J. & Hartmann, D. L. (2003). Eddy-Zonal Flow Feedback in the Northern Hemisphere Winter. *Journal of Climate*, Vol, 16, 1212–1227.

Monahan, A. H. & Fyfe, J. C. (2006). On the nature of zonal jet EOFs. *Journal of Climate*, Vol, 19, 6409–6424.

Palmer, T. (1999). A nonlinear dynamical perspective on climate prediction. *Journal of Climate*, Vol, 12, 575–591.

Rajeevan, M.; Bhate, J., Kale, J. D. & Lal, B. (2006). High resolution daily gridded rainfall data for the Indian region: Analysis of break and active monsoon spells. *Current Science*, Vol, 91, 296–306.

Silverman, B. W. (1981). Using kernel density estimates to investigate multimodality. *Journal of the Royal Statistical Society*, Vol, 43, 97–99.

Turner, A. G. & Hannachi, A. (2010). Is there regime behavior in monsoon convection in the late 20th century? *Geophysical Research Letters*, Vol, 37, doi:10.1029/2010GL044159.

Uppala, S. M. & Coauthors, (2005). The ERA-40 Re-Analysis. *Quarterly Journal of the Royal Meteorological Society,* Vol, 131, 2961–3012.

Webster, P. J. & Yang, S. (1992). Monsoon and ENSO−Selectivity interactive systems. *Quarterly Journal of the Royal Meteorological Society,* Vol, 118, 877–926.

Wittman, M. A. H.; Charlton, A. J. & Polvani, L. M. (2005). On the meridional structure of annular modes. *Journal of Climate*, Vol, 18, 2119–2122.

Woollings T.; Hannachi, A.; Hoskins, B. J. & Turner, A. G. (2010a). A regime view of the North Atlantic Oscillation and its response to anthropogenic forcing. *Journal of Climate,* Vol, 23, 1291–1307.

Woollings T.; Hannachi, A. & Hoskins, B. J. (2010b). Variability of the North Atlantic eddy-driven jet stream. *Quarterly Journal of the Royal Meteorological Society,* Vol, 136, 856–868.

Woollings, T., Pinto, J. G. & Santos J. A. (2011) Dynamical Evolution of North Atlantic Ridges and Poleward Jet Stream Displacements. *J. Atmos. Sci.*, 68, pp. 954-963.

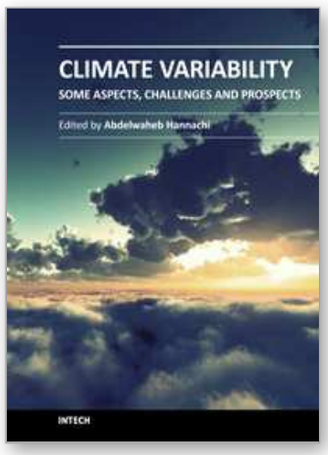

Climate Variability - Some Aspects, Challenges and Prospects
Edited by Dr. Abdel Hannachi

ISBN 978-953-307-699-7
Hard cover, 192 pages
Publisher InTech
Published online 18, January, 2012
Published in print edition January, 2012

This book provides a general introduction to the popular topic of climate variability. It explores various aspects of climate variability and change from different perspectives, ranging from the basic nature of low-frequency atmospheric variability to the adaptation to climate variability and change. This easy and accessible book can be used by professionals and non professionals alike.

How to reference
In order to correctly reference this scholarly work, feel free to copy and paste the following:

Abdel Hannachi, Tim Woollings and Andy Turner (2012). Atmospheric Low Frequency Variability: The Examples of the North Atlantic and the Indian Monsoon, Climate Variability - Some Aspects, Challenges and Prospects, Dr. Abdel Hannachi (Ed.), ISBN: 978-953-307-699-7, InTech, Available from: http://www.intechopen.com/books/climate-variability-some-aspects-challenges-and-prospects/atmospheric-low-frequency-variability-the-examples-of-the-north-atlantic-and-the-indian-monsoon

INTECH
open science | open minds

InTech Europe
University Campus STeP Ri
Slavka Krautzeka 83/A
51000 Rijeka, Croatia
Phone: +385 (51) 770 447
Fax: +385 (51) 686 166
www.intechopen.com

InTech China
Unit 405, Office Block, Hotel Equatorial Shanghai
No.65, Yan An Road (West), Shanghai, 200040, China
中国上海市延安西路65号上海国际贵都大饭店办公楼405单元
Phone: +86-21-62489820
Fax: +86-21-62489821

IntechOpen